

3-Dimensional Characterization of Ion Beam Current using a Hemispherical Sweep Apparatus

IEPC-2024-199

*Presented at the 38th International Electric Propulsion Conference
Pierre Baudis Convention Center • Toulouse, France
June 23-28, 2024*

C. Chhavi¹ and Mitchell L. R. Walker²
Georgia Institute of Technology, Atlanta, GA, 30332, USA

Abstract: Electric propulsion has become the favored approach for Low Earth Orbit (LEO) and orbit-raising maneuvers, resulting in a substantial expansion in its use in the satellite industry. The Hall effect thruster's (HETs) high specific impulse and thrust-to-power ratio allow for a wide range of in-space propulsion applications, making it a viable alternative for various space missions. Any manufacturing defect across various HET components can lead to disparity in plasma properties, subsequently affecting the performance of the thruster. In addition to altering the plasma parameters and the associated processes, these inconsistencies may cause a variation in the beam current and its subsequent deviance from the centerline, leading to thrust vectoring. Keeping in view the limitations of the complex electronic setups use of multiple probes utilized in previous studies evaluating thrust vectoring, a new design was proposed. A hemispherical sweep apparatus was designed and developed at the High-Power Electric Propulsion Laboratory School of Aerospace Engineering of the Georgia Institute of Technology, to characterize the three-dimensional plasma beam in terms of ion beam current. The apparatus's potential for investigating the thrust vectoring capabilities of thrusters was quantified by comparing ion beam current measurements with the conventional Faraday Probe scan, which was conducted exclusively in the horizontal direction. The sweep probe apparatus sweeps a Faraday probe vertically across the HET plume while spanning radially using a radial arm to gather three-dimensional ion currents. While taking measurements using hemispherical apparatus, three angular vertical sweeps of the Faraday probe ranging from -41° to 46° were performed consecutively to eliminate any systematic inaccuracy caused by the motion control system. The three-dimensional mapping of the plume revealed that the plume center was positioned at 4 deg below the center of the thruster, a different depiction of the plume center as opposed to that obtained through conventional horizontal sweep by the Faraday Probe. The ion beam current measured from the three-dimensional sweep probe apparatus exhibited a 0.03% decrease compared to the conventional horizontal scan, whereas the divergence angle showed a 4% variation. The apparatus was able to identify a 4° deviation of the plume in the vertical direction, highlighting plume asymmetry across the centerline. Due to its adaptability and simplicity, the design permits the attachment of diverse probes to acquire plasma properties at distinct locations within the plume. The sweep apparatus thus offers significant benefits in accurately measuring thruster performance, identifying plume non-uniformities, and tracking the thrust vector.

¹ Graduate Researcher, School of Aerospace Engineering, chhavi@gatech.edu, and AIAA Student Member

² Professor and Associate Dean, School of Aerospace Engineering, mitchell.walker@ae.gatech.edu, and AIAA Fellow.

Introduction

High effect thrusters (HETs) are electrostatic devices that accelerate the neutral particles of the propellant by ionizing them using an axial electric field and a radial magnetic field[1]. The acceleration of the ionized propellant particles out of the HET channel generate the necessary thrust for operational maneuvers[2]. An increasing number of satellite commercial operations are utilizing HET because of its uncomplicated design, high impulse, and high efficiency [3,4] [5]. The rising popularity of HET in the commercial sector contributes to its utilization in propulsion systems for Low Earth Orbit (LEO), Geosynchronous Earth Orbit (GEO), and interorbital missions[6–9].The thrusters are being mass-produced in response to the rising demand for HETs. Although it is relatively easy to produce thrusters in large quantities, yet it is crucial to conduct qualification testing to ensure that the HET meets the necessary performance and capability requirements for spaceflight operations. Present-day space missions necessitate propulsion devices with significant power and thrust capabilities. The mission objective is being accomplished by using HET in two separate manners. Firstly, by employing HET in a cluster arrangement to increase the propulsion system's thrust production[10,11]. Secondly, by developing larger HETs with multi-channel configurations that allow for enhanced propulsion capabilities[12–14]. Integrating mission and mass production requirements increases the likelihood that manufacturing defects will manifest in the HET components, resulting in their inability to complete flight qualification tests successfully. The presence of manufacturing defects across various HET components leads to disparities in plasma properties, which subsequently modify the thruster's performance parameters. In addition to altering the plasma parameters and the associated processes, these inconsistencies may cause a variation in the beam current and its subsequent deviance from the centerline, leading to thrust vectoring.

Several investigations have been carried out to examine and study the thrust vectoring capabilities of the thrusters during operation. Various thrust vector measurement systems have been developed utilizing the Faraday probe, double Langmuir, cylinder rods, and retarding potential analyzer (RPA) [15–20].Thrust vector characterization was conducted using four double-wired Langmuir probes aligned in the form of a cross situated 200cm downstream of the thruster exit plane[19] . A monitoring system utilizing reflective mirrors and charged couple device (CCD) cameras was employed to determine the thruster's centerline precisely. The movement of the ion beam centroid was traced using motorized position monitoring to detect any divergence in the thrust vector. The motorized mechanism was employed to maintain null error signals by equilibrating the current gathered in the two mutually perpendicular axes of the thrust vector measurement device, thereby enabling the tracking of the beam centroid. Nonetheless, the failure to detect the azimuthal unsymmetric condition and the unexplained systematic mistake leading to an overall thrust loss opened the door for additional research in this area. Polk designed a thrust vector probe comprising of 16 vertical and 16 horizontal graphite rods, each with a diameter of 9 mm and a length of 1.2 m[20]. The probe grid was positioned at the far end of the vacuum chamber, enabling uninterrupted beam exposure for long-term testing. A Leica Mancat theodolite system employed optical technology to precisely measure the alignment between the vector probe and the thruster axis[20]. An exhaustive analysis of the thrust vectoring condition for the Engineering Model Thruster (EMT2), which served as an engineering prototype of the NSTAR thruster, was conducted through 8000 hours of testing. The current obtained by the rods varied during the experiment. Possible causes of the initial thrust vector offsets, such as unsymmetric magnetic fields, have been identified but not thoroughly investigated. Nevertheless, this methodology proved effective in gathering rod current data that corresponded to ion beam current throughout an extended period of testing using an ion beamlet model [21]. Reijen[18] created another thrust vectoring device using RPA and energy-selective mass spectroscopy to analyze ion beam current and thrust vectoring. The thrust vector scanner comprised of 37 RPA mounted in a semicircle configuration on a pole. The boom was designed to provide data 1 m downstream of the thruster exit plane, allowing for far-field plume characteristics. The RPAs enabled the utility of ion selectability at a particular energy level, thereby permitting collections of ions of varying energy levels. Although the use of RPA enables greater accuracy, it necessitates more prolonged exposure to the plume, leading to the heightened deterioration of RPA grids. The RPA boom construction provided the ability to map the plasma plume fully. An alternative method, a thrust vectoring device comprised of an array of Faraday sensors that maps a portion of the ion beam, was devised by Benavides[15]. The device comprised of 23 Faraday probes affixed on a 1m curved aluminum framework installed on a motorized radial arm. The thrust vectoring device collected data ranging from -22° to 22° , encompassing approximately 44° of the plasma plume. The thruster vectoring device successfully generated a comprehensive three-dimensional map of the ion beam at various operating conditions for the Advanced Electric Propulsion System (AEPS) HET. The apparatus enabled precise measurements of the beam current and thrust vector while preventing any escalation in the back sputter effect on the thruster.

To overcome the limitations of complex electronic setups with multiple probes and to achieve a broader ion beam coverage, a hemispherical sweep apparatus has been developed. This apparatus, designed to provide the characteristics of a three-dimensional plasma beam, offers a comprehensive measurement setup for plasma non-uniformities and potential use in studying the thrust vectoring capabilities of thrusters. The equipment sweeps a Faraday Probe vertically across the HET plume while spanning radially using a radial arm to gather three-dimensional ion currents. In this paper, the device is utilized to validate the current approach to HET plume characterization. Specifically, it characterizes the ion beam current of a 5-kW laboratory HET, P5[22], operating in uniform magnetic field configuration demonstrating the precise position of the thruster vector in three-dimensional space.

Design Overview

A. Design Objective

The objective of the current hemispherical sweep probe apparatus is to provide three-dimensional plume characterization of the HET plasma plume in terms of the ion beam current. The three-dimensional mapping of the ion beam current is provided using the Faraday probe as the primary ion beam current measuring device in the apparatus. For this undertaking, the subsequent objectives and requirements are identified:

- 1) The diagnostic apparatus enables precise and repeatable characterization to facilitate plume measurement.

The objective emphasizes the need for precise and dependable measurement with less than 2° deviations. The criteria are derived from the guidelines outlined in the recommended practices for precise measurements utilizing the Faraday Probe[23]. This criterion restricts measurement uncertainty to less than 2° , enabling the translating mechanism to operate with minimal tremble and optimum position control.

- 2) Orthogonality must be maintained between the probe collector surface and the ion beam.

The current objective necessitates that the probe collection surface remains orthogonal to the plume to maximize the surface area for ion beam current collection. Additionally, it promotes the reduction of sheath potential effects that occur when ions interact with the collector plate.

- 3) Capability to provide continuous sweep measurements throughout extended periods of testing.

The objective enables the probe setup to be used for many tests over a long period of time, with the ability to withstand considerable temperature and pressure variations in the vacuum facility environment. The requirement necessitates that the probe instrument possesses robustness and longevity to ensure its sustained utilization in the future.

- 4) The impact of the probe's presence in the plume on the floating potential of the thruster is negligible.

This objective aims to provide guidance for designing the sweep probe apparatus to minimize its impact on the plasma and the thruster operating conditions, ensuring accurate plasma performance characteristics.

- 5) Capability to regulate the frequency of measurement or data sweeps of the plume.

The capacity to regulate the frequency of measurements facilitates the acquisition of comprehensive and spatially specific data at the intended locations of interest. The sweep probe apparatus enables the operator to collect more extensive data sets in concentrated areas, such as the centerline for thrust vectoring or plume endpoints for facility effects.

- 6) A lightweight, simplistic design featuring minimal back sputtering.

The simplistic, lightweight design of the sweep probe apparatus allows for easy installation and utilization of the setup for various testing conditions. It also increases the data collection capabilities of the testing facility, aiding in the advancement of the understanding of the plasma plume.

B. Design

The design objective provides a detailed requirement needed to be fulfilled by the sweep probe apparatus for successful validation and utilization. These goals are accomplished by the current apparatus consisting of a geared face curved framework/track, a motion-controlled gear, a probe mount, and probe electronics incorporated into the sweep probe apparatus to enable the probe to be swept across the plasma plume. Due to its adaptability and simplicity, the design permits the attachment of diverse probes to acquire plasma properties at distinct locations within the plume. The current design utilizes a Faraday probe to detect the ion beam current across the plume.

The apparatus consists of a circular framework with a radius of 1 meter, constructed from lightweight aluminum, as depicted in Fig 1. The framework is composed of a geared track on one side and a curved flat surface insulated from the plume using graphite fragments on the other side. A slot is created in the aluminum structure to accommodate motion bearings and preserve the orthogonality of the probe while moving along a curved trajectory. The bearing linked to the probe mount guarantees that the probe remains in the correct orientation while sweeping through the plume. The geared track framework currently ranges from -41 to 46° , providing a measurement span of 87° of the plume. The framework can be extended to 180° span in facilities without spatial restrictions such as floor and the thruster mount. The probe mount is fabricated utilizing a combination of aluminum and graphite components. The aluminum brackets are connected with the motion gear as well as the stepper motor employed for motion control. As depicted in Figure , the Nema 17 motor with a 50:1 ratio planetary gearbox is utilized to translate the probe along a 1m radius path via a motion gear. The stepper motor enables accurate gear movement along the track and provides positional control over the probe. The graphite component of the mount serves the purpose of connecting the Faraday probe to the mount while guaranteeing electrical isolation and reduced interference during measurements as seen in Fig 2. The construction of the Faraday probe adheres to the recommended principles, utilizing a stainless steel casing that is 1 inch in length and a collector coated with tungsten[23].

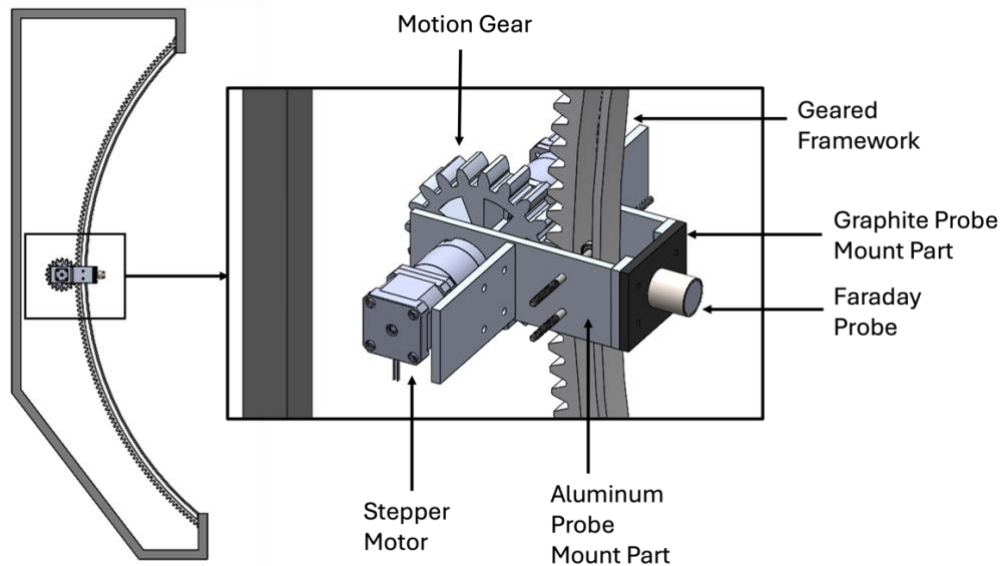


Figure 1 - Detailed rendering of the 1-m Curved Sweep probe apparatus with its components a) Stepper motor b) Motion control gear c) Gear framework d) Faraday probe and e) Aluminum and Graphite Mount components

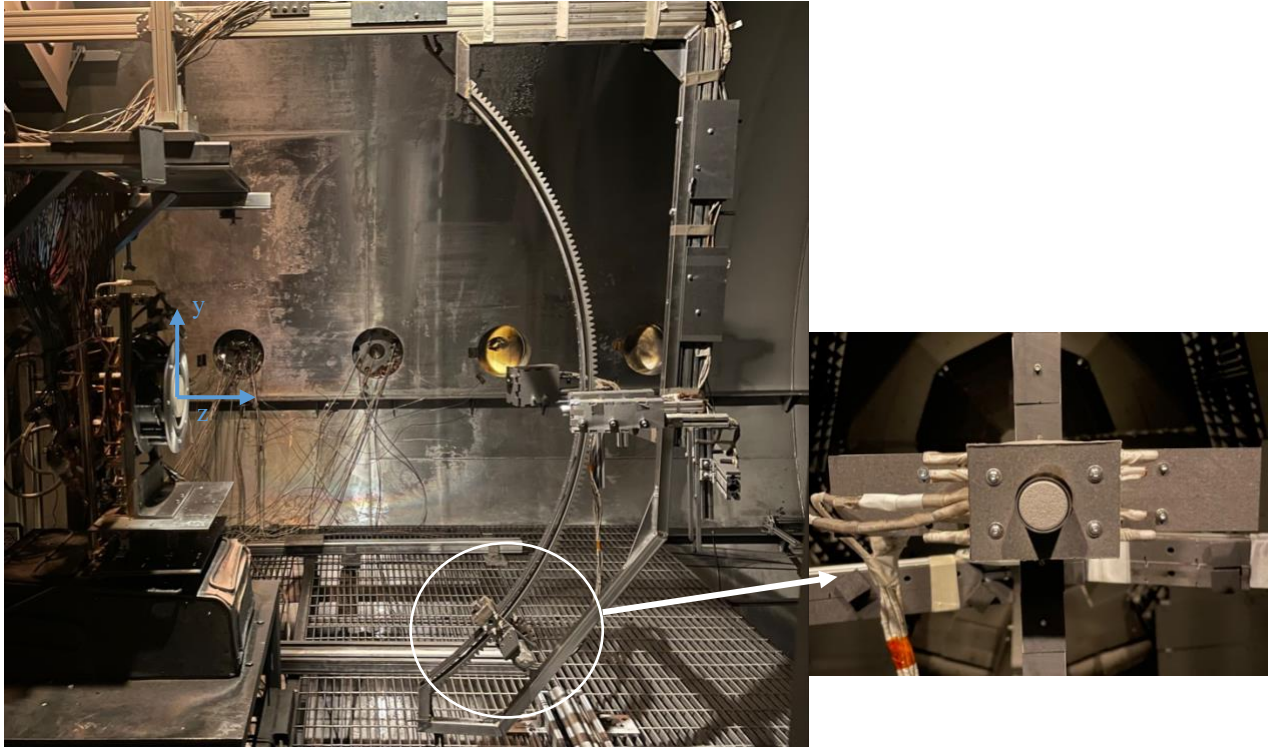


Figure 2 - Picture of the 1-m Curved Sweep Probe Apparatus installed in VTF-2.

Experiment Procedure

A. Vacuum Facility

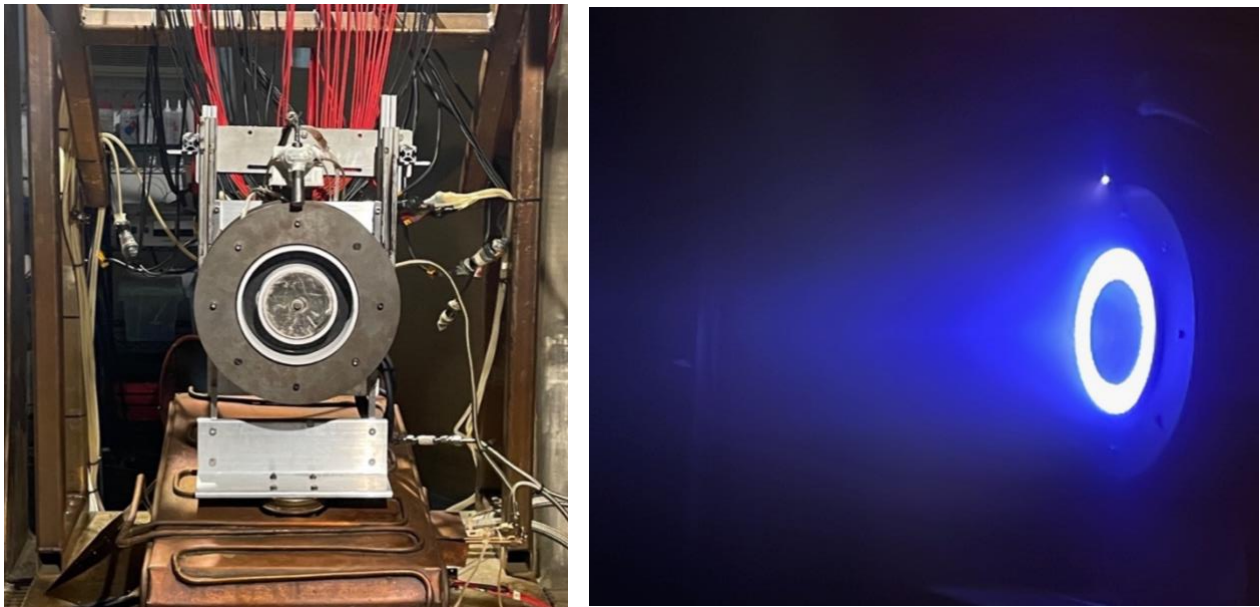
All investigations are conducted in Vacuum Test Facility 2 (VTF-2) in the High-Power Electric Propulsion Laboratory of the Georgia Institute of Technology. VTF2 consists of a 9.2 m long stainless steel chamber with a diameter of 4.9m[24]. High vacuum is attained using ten liquid nitrogen-cooled CVI TM1200i cryopumps linked to two Stirling Cryogenics SPC-4 compressors. The pressure is measured using one Agilent Bayard-Alpert (BA) 571 hot-filament ion gauges on the chamber flange and two MKS Granville Phillips 370 Stabil-ion gauges located 0.3 m downstream of the thruster exit plane and 0.6m from the thruster centerline. The Agilent XGS-600 Gauge Controller is utilized to regulate the outer ion gauge and Granville Phillips 370 Controller was used for the ion gauges inside the chamber to deliver precise pressure measurements. During testing, the ion gauge inside the chamber recorded nominal operating pressures of 5.9×10^{-6} Torr- N_2 and, 1.1×10^{-5} Torr- N_2 , respectively. The operational and base pressures were measured and then averaged using two gauges. Subsequently, the operational pressure was adjusted for krypton using a correction method.

$$p_{\text{operational-corrected}} = \frac{1}{\text{corr}}(p_{\text{operational-measured}} - p_{\text{base}}) + p_{\text{base}}, \quad (1)$$

with *corr* being equal to 1.96 for krypton[25]. Resulting in the base and operational pressure in the facility being equal to 2.55×10^{-9} Torr- N_2 and 3.1×10^{-6} Torr-Kr.

B. 5-kW Hall Thruster

The experiment presented in this study was conducted using a 5-kW laboratory HET P5, built in 1997, through a collaboration between the Air Force Research Laboratory (AFRL) and the University of Michigan. The P5 HET was used for the experiment due to its comparable performance capabilities to commercial HETs [22]. P5 features a stainless-steel anode with 36 slot holes, a ceramic discharge channel, an inner magnetic core, and eight outside magnetic cores that generate the magnetic field necessary for the functioning of the HET. The thruster comprises a boron nitride and silicon dioxide BN-SiO₂, M26 grade channel with an outside diameter of 173 mm and breadth of 25 mm[26,27]. The magnetic circuit architecture of eight outer cores form the outer coil circuit and one inner coil. A hollow cathode of EPL-500 was positioned at a distance of 2.2 cm downstream of the P5 exit plane and 7 cm above the centerline, as depicted in Figure . The thruster was operated at a discharge voltage of 300 V, an anode flow rate of 5.61mg/s, and a cathode flow rate of 0.44 mg/s of krypton.



a) b)
**Figure 3 - a) P5 Thruster with externally mounted EPL-500 cathode mounted on VTF-2 thrust stand.
b) P5 operating at 2.3-kW condition on krypton.**

C. Hemispherical Sweep Apparatus

The aluminum track hemispherical apparatus had a 1 m radius and was powered by a stepper motor that achieves a step size of 1.8° per step. The Ni motion controller MID-7604/7602 allowed for the adjustment of the motor's speed during operation. A stepper motor is employed in conjunction with limit switches positioned at the endpoints to monitor the probe's location as it moves along a curved path. At -45 and 50° from the track, high-precision limit switches are arranged so that the probe mount contact can activate the limit switch circuit and halt the stepper's motion. The entire sweep probe apparatus is positioned on a radial probe arm, so that there is a 1m distance between the probe collector and the thruster exit plane in VTF-2, as seen in Figure 3. The radial probe arm is designed to undergo a sweeping motion, starting from -90° and ending at 90° with a velocity of 0.63° per second. The probe arm is controlled by a Parker Daedal 200RT series rotary table, which has an accuracy of $\pm 17^\circ$ [28], as depicted in Figure . The angular transverse motion and the stepper motor-driven vertical motion of the Faraday probe are controlled by Agilent 34970A

Data Acquisition Unit (DAQ). LabVIEW Virtual Instrument is used to record both the probe location and the ion beam current gathered by the Faraday probe.

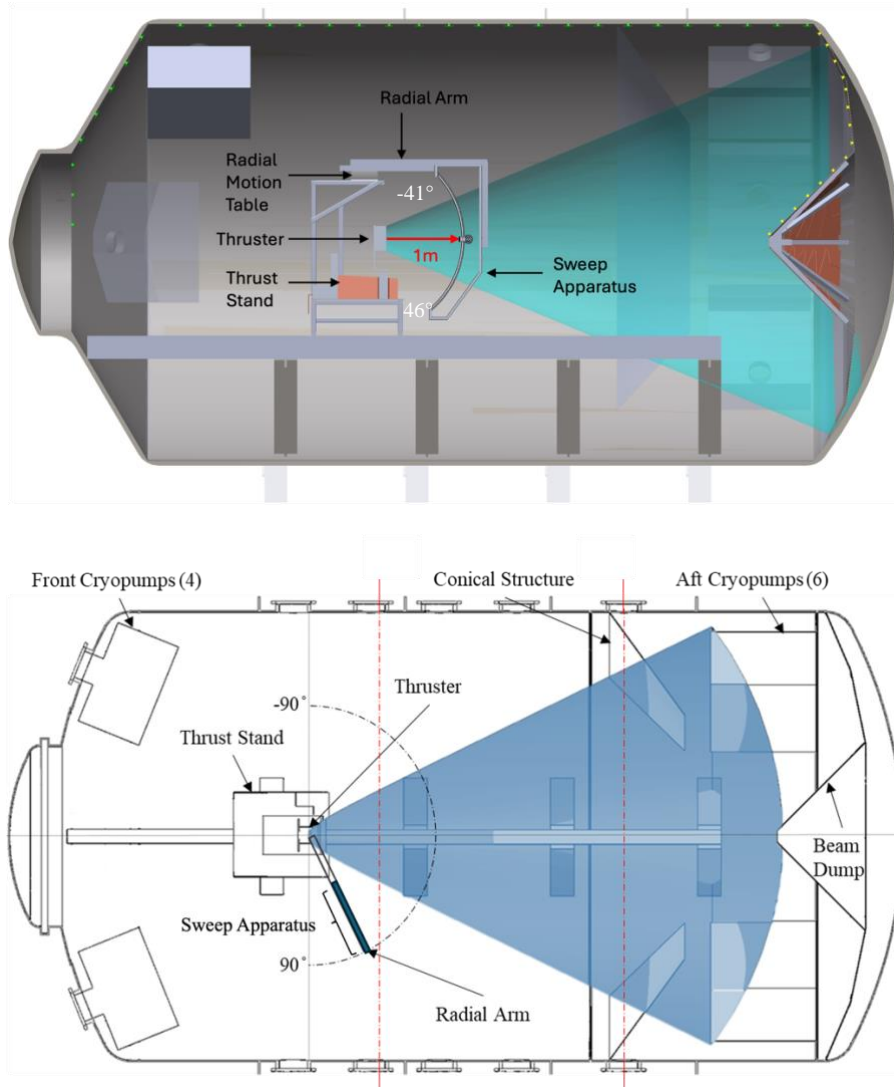


Figure 4 - Schematic orientation of the Sweep probe apparatus with respect to P5 in VTF-2 chamber.

The P5 thruster was powered by a voltage of 300 V, with the outer coil current and inner coil current set to 4 A and 6 A, respectively. The thruster is run for three hours before reaching a thermal steady state displayed by a rate of change of thruster temperature of less than 0.5 °C/min. After the thruster reaches a thermal steady state, a conventional Faraday probe mounted on the radial arm is utilized to take ion beam current measurements with a horizontal sweep from -90° to 90° for comparison of ion beam current obtained through the measurements taken with hemispherical sweep apparatus. The guard and collector of the Faraday probe are biased at -30 V based on the recommended practices [23]. While taking measurements using hemispherical apparatus, three angular vertical sweeps of the Faraday probe are performed consecutively in opposite directions (-41 to 46°, 46 to -41° and again -41 to 46°) to eliminate any systematic inaccuracy caused by the motion control system. Following three vertical sweeps with the sweep apparatus, the probe arm is repositioned in a radial direction to conduct a vertical scan at the next horizontal position. Measurements are collected at intervals of 5° in the horizontal direction in the main plume, near the centerline. The

duration to perform the mapping of the entire plume region is two hours. The collected data is subsequently examined utilizing the correction factors and methodologies outlined by Brown[29]. The method mentioned has an error of around 5% for the beam current and 1.5% for the plume divergence half-angle[23,30].

Results and Discussion

The P5 Hall thruster, operating at a voltage of 300 V, with an anode flow rate of 5.61 mg/s and a cathode flow rate of 0.44 mg/s, generated a discharge current of 7.90 A, resulting in an operational power of 2.3 kW. A comparison was made between the ion beam currents measured using a typical Faraday probe setup and a hemispherical sweep apparatus to comprehend the extent of variations in the measurements as seen in Fig.6. The standard setup for a Faraday probe involves attaching it to a radial arm and performing a horizontal sweep across the plume, covering an angle range from -90° to 90° . After three successive scans, the plume's horizontal sweep showed an ion beam current of 4.11 A and a divergence half angle of 33.23° for the P5 at 2.3-kW condition. The computed ion beam current incorporates the necessary adjustments for secondary electron emissions and charge exchange collisions and is expressed as 95% of the total ion beam current. The traditional method relies on numerous assumptions, along with the assumption of the axisymmetric magnetic field to obtain ion beam current. Nevertheless, this method is deemed inapplicable for operating conditions that exhibit unsymmetric plume characteristics and unsymmetrical magnetic field conditions.

An examination of variations in plume behavior was conducted by performing a vertical sweep down the centerline using the sweep probe apparatus, with the horizontal position fixed at 0° . The vertical sweep ranged from -41° to 46° , as depicted in Fig. 5. Following the three successive sweeps, the ion beam current obtained was 4.73 A. The multiple scans conducted using the hemispherical apparatus yielded a standard error of 1.8×10^{-7} , indicating highly repeatable measurements. The comparison between the two alternative configurations was hindered by data variances caused by systematic error, which arose from employing two different Faraday probes for horizontal and vertical scans to measure ion current. Therefore, a horizontal scan was conducted utilizing a Faraday probe on the sweep equipment in a centerline arrangement at a constant 0° vertical position. The horizontal scan displayed ion current data at 5° intervals due to the probe's operational configuration. The horizontal scan obtained using the sweep apparatus enabled a more efficient vertical and three-dimensional sweep comparison. However, an interval of 5° allowed for a loss in measurement accuracy [23]. The horizontal scan of the sweep apparatus yielded a 95% ion beam fraction of 5.71A and a half divergence angle of 35.39° . To make a more precise comparison with data from the horizontal sweep, measurements from the horizontal scan for angles -90° to -41° and 46° to 90° were extracted and scaled to fit the vertical scan, allowing extrapolation of ion current densities to -90° and 90° , as shown in Fig. 5. As illustrated in Fig. the extrapolated vertical scan adhered the trend of ion current density variation with sweep angles similar to horizontal scan. The ion beam current fraction from the vertical scan was calculated to be 6.11 A after extrapolation, with a divergence angle of 35.32° . The analysis of the ion beam currents during horizontal and vertical scans revealed a 6% rise in ion beam current. The asymmetrical plume was initially attributed to the externally located cathode used to operate the P5. However, additional measurements with a centrally mounted cathode would provide further insight into the cause of the variation in the plume measurements. The discrepancies in ion beam current calculations necessitated using a three-dimensional mapping technique to obtain more precise plasma characteristics and plume asymmetry measurements.

The hemispherical sweep probe apparatus performed observations with a horizontal separation of 5° while scanning vertically from -41° to 46° to obtain three-dimensional ion current measurements. Three consecutive vertical scans with a standard error of 1.8×10^{-7} provided highly accurate results. While conducting vertical scans at various horizontal positions, ion current scans at the extremities, namely -90° and 90° horizontal positions, diverged significantly from the trends found at the centerline. The ion current at the two extreme locations exhibited a linear variation with the angular sweep, as illustrated in Fig.7. The examination of the facility depicted in Fig 3a) allowed for the assessment of the presence of propellant lines at the 90° angle horizontal position, as well as the metallic thrust structure at both locations, as a potential cause for the higher electrical currents observed at the wings compared to the center during a vertical scan. Though the measurements at the extremities are 100 times lesser in magnitude compared to the center of the thruster, the impact of structural components located close to the thruster on the plume was demonstrated. The sweep probe apparatus was the sole effective tool for observing these effects and providing findings for future research.

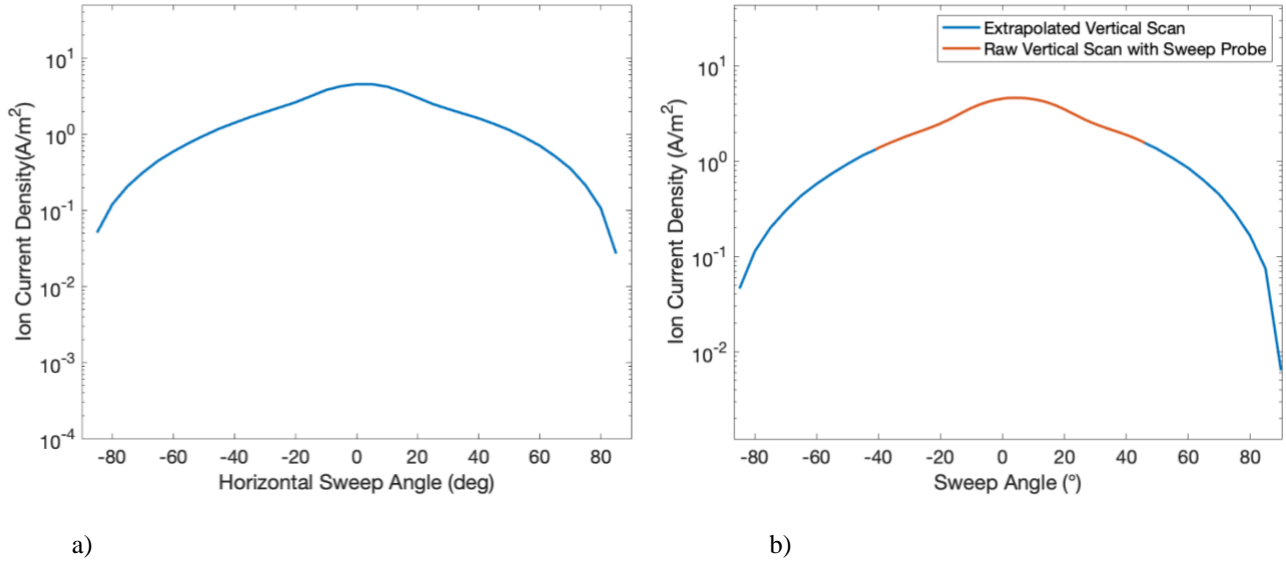


Figure 5 - a) Ion current as a function of horizontal sweep angle b) extrapolated ion current as a function of vertical sweep angle at 300 V and 7.90 A with anode mass flow of 5.61mg/s and cathode mass flow of 0.44mg/s.

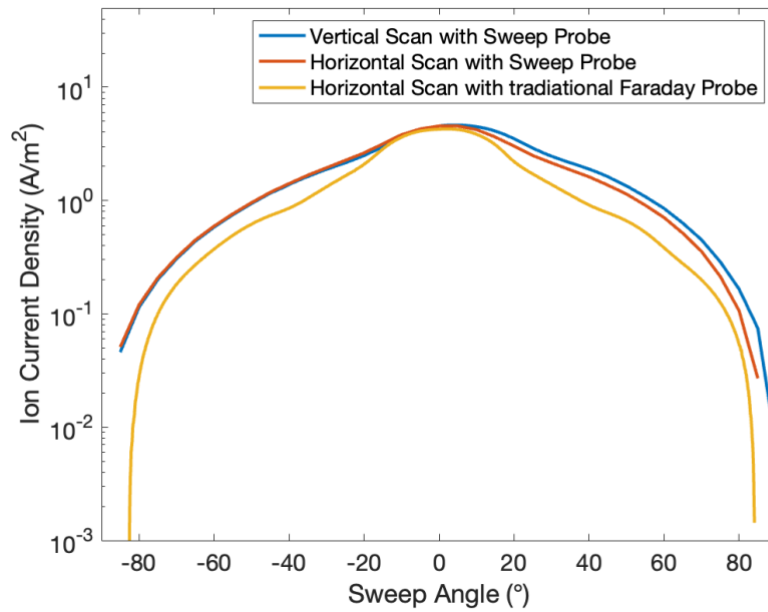


Figure 6 - Ion current density as a function of angle with 1) horizontal sweep using the traditional Faraday probe 2) horizontal sweep using sweep probe apparatus 3) extrapolated vertical scan using sweep probe apparatus for P5 operating at 300 V and 7.90 A with anode mass flow of 5.61mg/s and cathode mass flow of 0.44mg/s.

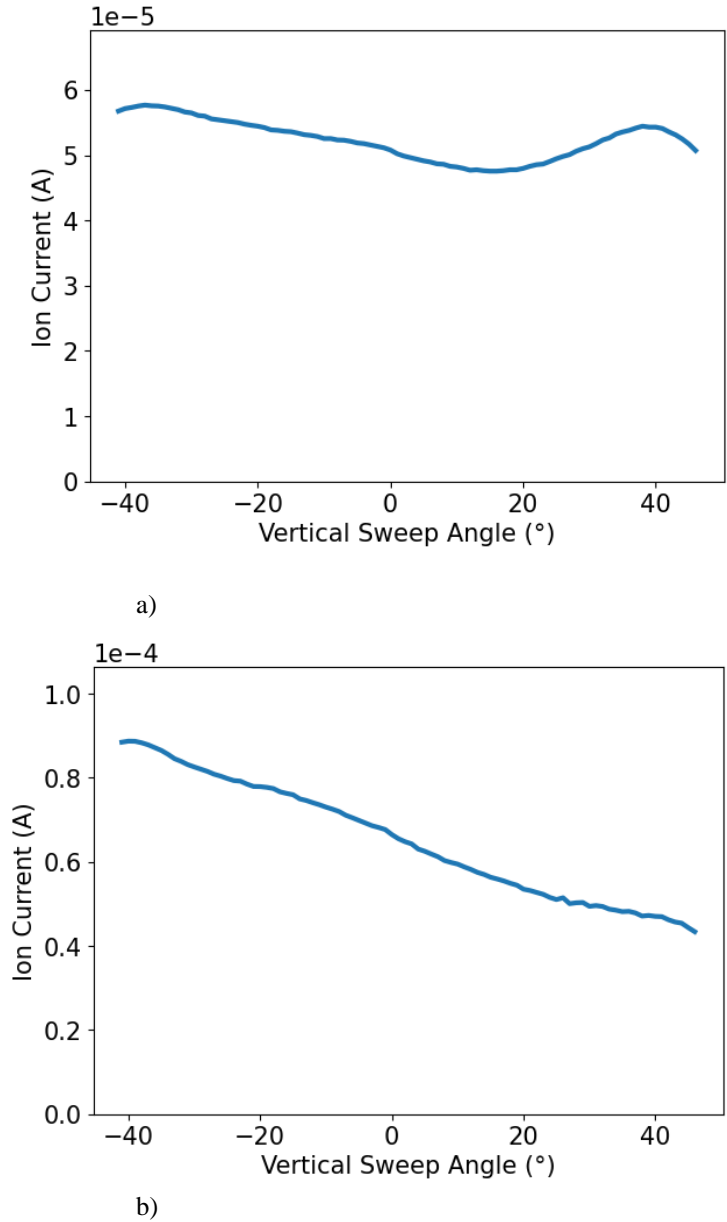
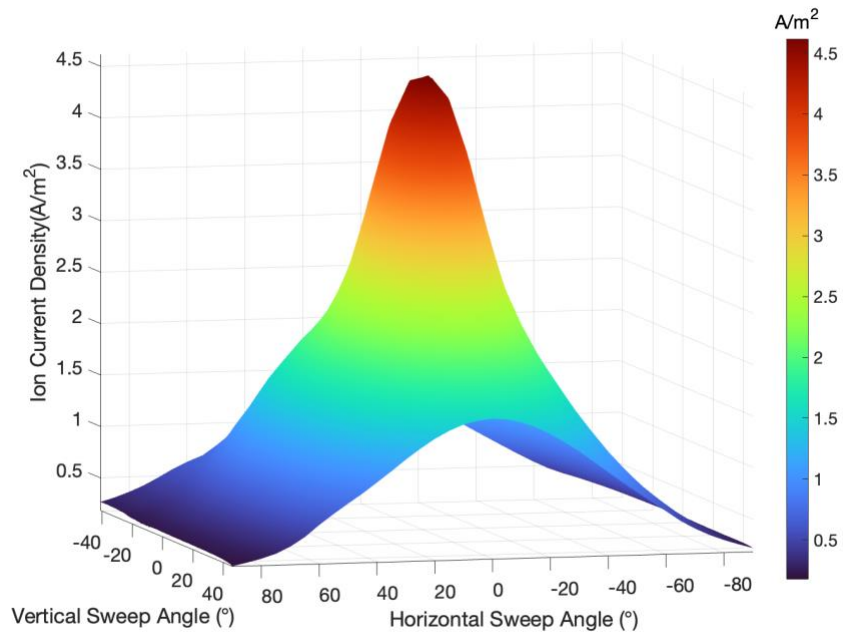
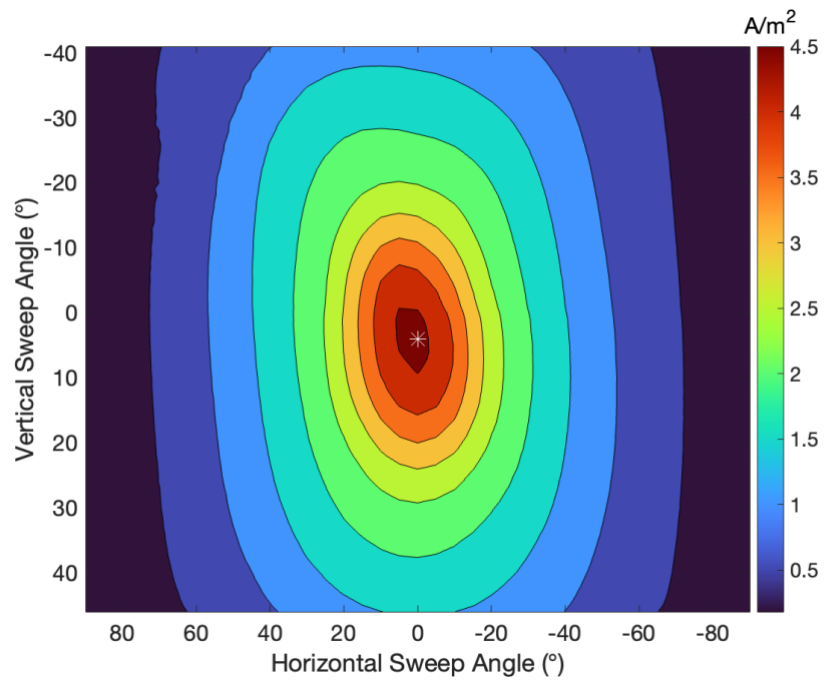


Figure 7 - Measured ion current as a function of angle for a) Vertical scan at -90° horizontal position b) Vertical scan at 90° horizontal position.

Ion current collected through the full 3-dimensional mapping is illustrated in Fig. 8. The analysis of the raw data from the three-dimensional sweep yielded an estimated ion beam current of 3.60 A, accompanied by a divergence angle of 26.03° . The data was corrected for secondary electron emission and charge exchange in the horizontal direction, as the vertical sweep was restricted to -41° to 46° . The hemispherical scan yielded a 36.9% decrease in the measurement of ion beam current due to the restricted vertical sweep range. The vertical scans were extrapolated using the horizontal scan measurements to determine the potential full-scale measurement of the ion beam current while preserving the trend of ion current density variation across the 37 vertical scans. The data extrapolation resulted in measurements that span from -90° to 90° in both the vertical and horizontal directions, thereby enabling the total estimation of the hemispherical ion current for P5 at 2.3 kW, as illustrated in Fig. 9.

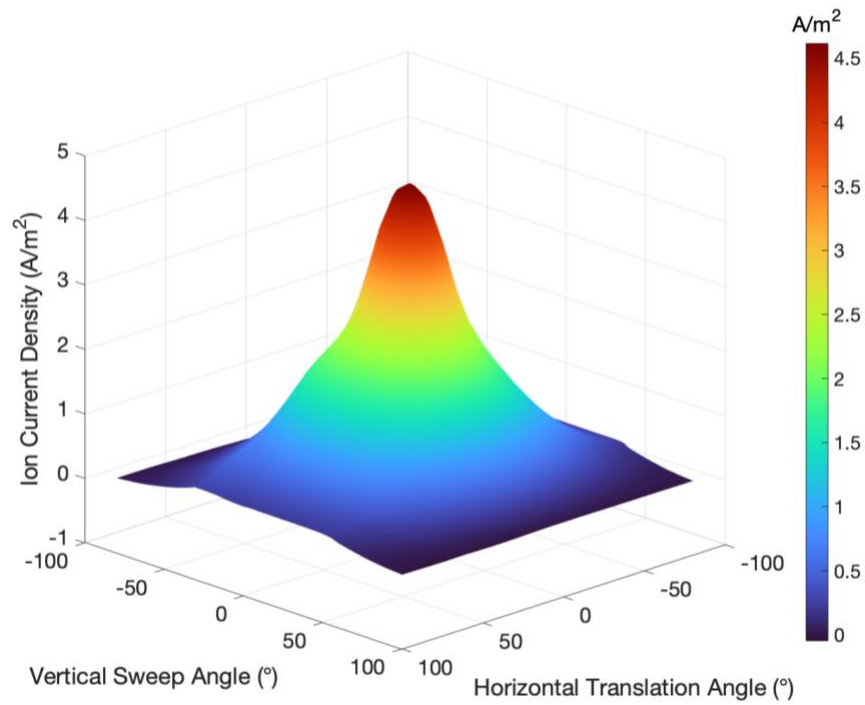


a)

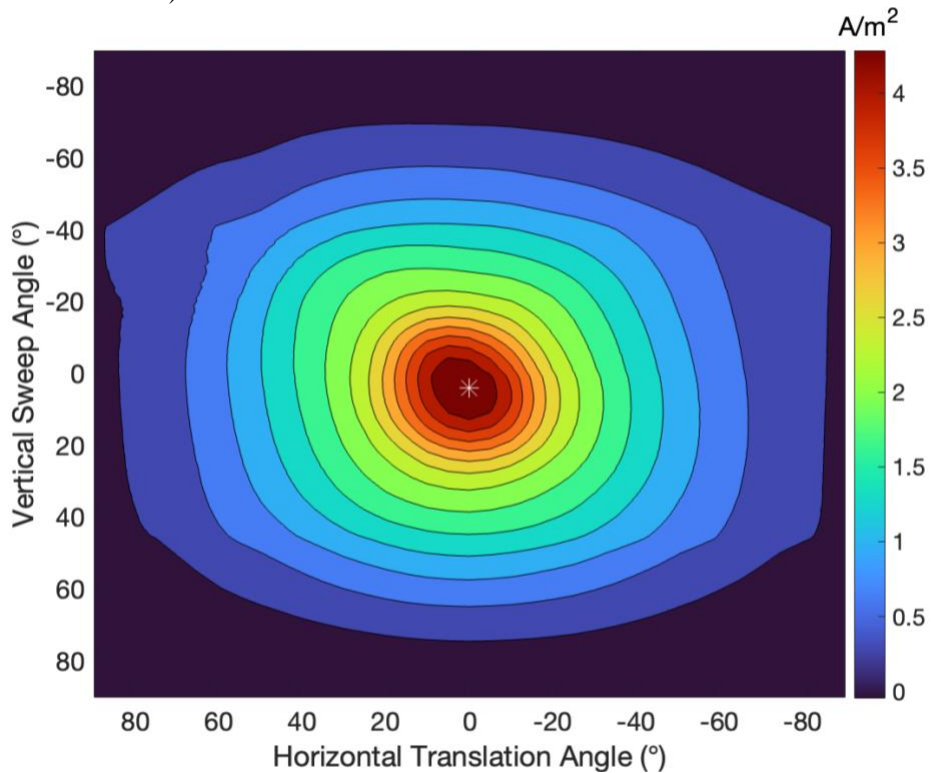


b)

Figure 8 - a) 3-Dimension ion current variation with horizontal and vertical sweep b) Contour map of ion current depicting the position of the plume center



a)



b)

Figure 9 - a) 3D ion current variation containing extrapolated measurements with horizontal and vertical sweep b) Contour map of ion current density containing extrapolated measurements depicting the position of the plume center.

An ion beam current measurement of 5.71 A and a divergence angle of 33.94° was obtained from the extrapolated three-dimensional ion current. The ion beam current measurements were evaluated after correcting for secondary electron emission and charge exchange at horizontal and vertical angles, yielding a 95% ion beam percentage. The hemispherical sweep mechanism had a negligible effect on the floating potential of the thruster, allowing it to be used without impacting its operation. The measurements acquired with the hemispherical apparatus were subject to uncertainty. This uncertainty included a $\pm 10\%$ margin of error connected with the Faraday probe[23] and a margin of error of less than $\pm 1\%$ associated with the gear motion control system for vertical scan and a $\pm 2\%$ for the horizontal motion control system. The current peak's position was determined and tracked using three-dimensional plume mapping to predict the position of the thrust vector. The maximum value of the ion current was observed to occur at the center line of the thruster in the horizontal sweep direction, which was consistent with the horizontal sweep direction observed using the conventional Faraday probe device. The vertical scan, as well as the three-dimensional scan, offered an alternative representation of the position of the thrust vector. The plume center was located 4 degrees below the center of the thruster. The capacity to provide high-resolution vertical scans with measurements taken at 0.1° intervals made such plume characterization possible and provided excellent tracking capabilities. The three-dimensional probe device offered additional validation for its potential application as a measurement tool for tracking the thrust vector of the HET plume. This instrument can be utilized to test thrusters with vectoring capabilities and to examine the effects of clustering thrusters at different positions on the direction of the thruster vector. Table 1 showcases the ion beam current and half divergence angle achieved through different sweeping directions/configurations. The ion beam current measured from the three-dimensional sweep probe apparatus exhibited a 0.03% decrease compared to the horizontal measurement made using the sweep apparatus, whereas the divergence angle only showed a 4% variation. While the three-dimensional sweep probe apparatus yielded a beam current only 0.03% less than the horizontal scan, the differences in the plume parameter indicated an increase in measurement accuracy in comparison to a two-dimensional scan of the plume. The sweep apparatus offered significant benefits in accurately measuring thruster performance, identifying plume non-uniformities across horizontal and vertical, and tracking the thrust vector. The sweep apparatus potential utilization for ion current measurement at point of non-uniformities in the plasma in future experiments will highlight the importance of instrument and allow better quantification of the accuracy of the measurements.

Table 1 - Ion beam current and beam divergence for different sweep probe apparatus measurement configurations at 300 V and 7.90 A

Sweep probe apparatus Configuration	Ion beam Current (A)	Half Divergence Angle (°)
Horizontal Sweep	5.71	35.39
Vertical Sweep without extrapolation	4.73	24.42
Vertical Sweep with extrapolation	6.11	35.32
3D Sweep without extrapolation	3.60	26.03
3D Sweep with extrapolation	5.71	33.94

Conclusion

The hemispherical sweep apparatus demonstrated the three-dimensional measurement of ion current across the HET distribution. The apparatus allows the user to monitor and quantify non-uniformities in the plasma plume and trace the thrust vector. The hemispherical sweep probe apparatus can be used with different probe mount modifications to achieve distinct plasma characteristics at other positions. The present work employed the hemispherical sweep apparatus equipped with a Faraday probe to get precise measurements of ion beam current. This sweep apparatus yielded a 0.03% decrease in ion beam current compared to the horizontal sweep measurements. The mapping of the plume illustrates the importance of the hemispherical sweep equipment in obtaining greater precision in measurements of plume parameters without interfering with thruster operation. The thruster vector tracking capabilities of the sweep apparatus also enabled the discovery of vertical asymmetry of the P5 HET plume, with an inclination of 4° while maintaining the horizontal symmetry. The hemispherical apparatus's potential for observing thruster plume non-uniformities and tracking thrust vectors for HET and HET clusters opens new possibilities for future electric propulsion research.

References

- ¹Jahn, R. G., "Physics of Electric Propulsion," Dover Publ, Mineola, NY, 2006.
- ²Goebel, D. M., and Katz, I., "Fundamentals of Electric Propulsion: Ion and Hall Thrusters," Wiley, 2008. <https://doi.org/10.1002/9780470436448>
- ³Hofer, R., and Gallimore, A., "High-Specific Impulse Hall Thrusters, Part 2: Efficiency Analysis," *Journal of Propulsion and Power - J PROPUL POWER*, Vol. 22, 2006, pp. 732–740. <https://doi.org/10.2514/1.15954>
- ⁴O'Reilly, D., Herdrich, G., and Kavanagh, D. F., "Electric Propulsion Methods for Small Satellites: A Review," *Aerospace*, Vol. 8, No. 1, 2021, p. 22. <https://doi.org/10.3390/aerospace8010022>
- ⁵Lev, D., Myers, R. M., Lemmer, K. M., Kolbeck, J., Koizumi, H., and Polzin, K., "The Technological and Commercial Expansion of Electric Propulsion," *Acta Astronautica*, Vol. 159, 2019, pp. 213–227. <https://doi.org/10.1016/j.actaastro.2019.03.058>
- ⁶Bapat, A., Salunkhe, P. B., and Patil, A. V., "Hall-Effect Thrusters for Deep-Space Missions: A Review," *IEEE Transactions on Plasma Science*, Vol. 50, No. 2, 2022, pp. 189–202. <https://doi.org/10.1109/TPS.2022.3143032>
- ⁷Raites, Y., Guelman, M., Ashkenazy, J., and Appelbaum, G., "Orbit Transfer with a Variable Thrust Hall Thruster Under Drag," *Journal of Spacecraft and Rockets*, Vol. 36, No. 6, 1999, pp. 875–881. <https://doi.org/10.2514/2.3506>
- ⁸Misuri, T., Pergola, P., and Andrenucci, M., "HT5k Hall Thruster to Improve Small Launcher Capabilities," presented at the In Proc. 33rd International Electric Propulsion Conference, 2013.
- ⁹Jackson, J., Cassady, J., Allen, M., Myers, R., Tofil, T. A., Herman, D. A., and Pencil, E. J., "Development of High Power Hall Thruster Systems to Enable the NASA Exploration Vision," presented at the 2018 Space Propulsion Conference, Seville, 2018.
- ¹⁰Victor, A. L., Zurbuchen, T. H., and Gallimore, A. D., "Ion-Energy Plume Diagnostics on the BHT-600 Hall Thruster Cluster," *Journal of Propulsion and Power*, Vol. 22, No. 6, 2006, pp. 1421–1424. <https://doi.org/10.2514/1.20514>
- ¹¹Beal, B. E., Gallimore, A. D., Haas, J. M., and Hargus, W. A., "Plasma Properties in the Plume of a Hall Thruster Cluster," *Journal of Propulsion and Power*, Vol. 20, No. 6, 2004, pp. 985–991. <https://doi.org/10.2514/1.3765>
- ¹²Hall, S. J., Jorns, B. A., Cusson, S. E., Gallimore, A. D., Kamhawi, H., Peterson, P. Y., Haag, T. W., Mackey, J. A., Baird, M. J., and Gilland, J. H., "Performance and High-Speed Characterization of a 100-kW Nested Hall Thruster," *Journal of Propulsion and Power*, Vol. 38, No. 1, 2022, pp. 40–50. <https://doi.org/10.2514/1.B38080>
- ¹³Liang, R., "The Combination of Two Concentric Discharge Channels into a Nested Hall-Effect Thruster.," Ph.D. dissertation, University of Michigan, 2013.
- ¹⁴Duchemin, O., and Valentian, D., "Thrust Vector Control Using Multi-Channel Hall-Effect Thrusters," presented at the 43rd AIAA/ASME/SAE/ASEE Joint Propulsion Conference & Exhibit, Cincinnati, OH, 2007. <https://doi.org/10.2514/6.2007-5203>
- ¹⁵Benavides, G. F., Mackey, J., Ahern, D., and Thomas, R., "Diagnostic for Verifying the Thrust Vector Requirement of the AEPS Hall-Effect Thruster and Comparison to the NEXT-C Thrust Vector Diagnostic," presented at the 2018 Joint Propulsion Conference, Cincinnati, Ohio, 2018. <https://doi.org/10.2514/6.2018-4514>
- ¹⁶Sohl, G., and Fosnight, V. V., "Thrust Vectoring of Ion Engines.," *Journal of Spacecraft and Rockets*, Vol. 6, No. 2, 1969, pp. 143–147. <https://doi.org/10.2514/3.29552>
- ¹⁷HOMA, J., and WILBUR, P., "Ion Beamlet Vectoring by Grid Translation," *16th International Electric Propulsion Conference*, American Institute of Aeronautics and Astronautics. <https://doi.org/10.2514/6.1982-1895>
- ¹⁸Van Reijen, B., Weis, S., Lazurenko, A., Haderspeck, J., Genovese, A., Holtmann, P., Ruf, K., and Püttmann, N., "High Precision Thrust Vector Determination through Full Hemispherical RPA Measurements Assisted by Angular Mapping of Ion Energy Charge State Distribution," 2013.
- ¹⁹Pollard, J., and Welle, R., "Thrust Vector Measurements with the T5 Ion Engine," *31st Joint Propulsion Conference and Exhibit*, American Institute of Aeronautics and Astronautics. <https://doi.org/10.2514/6.1995-2829>

²⁰Polk, J., Anderson, J., and Brophy, J., “Behavior of the Thrust Vector in the NSTAR Ion Thruster,” *34th AIAA/ASME/SAE/ASEE Joint Propulsion Conference and Exhibit*, American Institute of Aeronautics and Astronautics. <https://doi.org/10.2514/6.1998-3940>

²¹Haag, Thomas, “Translation Optics for 30 Cm Ion Engine Thrust Vector Control,” IEPC-01-116, 2002.

²²Gulczinski, Frank, “Examination of the Structure and Evolution of Ion Energy Properties of a 5kW Class Laboratory Hall effect Thruster at Various Operational Conditions,” University of Michigan, 1999.

²³Brown, D. L., Walker, M. L. R., Szabo, J., Huang, W., and Foster, J. E., “Recommended Practice for Use of Faraday Probes in Electric Propulsion Testing,” *Journal of Propulsion and Power*, Vol. 33, No. 3, 2017, pp. 582–613. <https://doi.org/10.2514/1.B35696>

²⁴Kieckhafer, A. W., “Recirculating Liquid Nitrogen System for Operation of Cryogenic Pumps,” presented at the 32nd International Electric Propulsion Conference, Electric Rocket Propulsion Society, Wiesbaden, Germany, 2011.

²⁵Dushman, S., “Scientific Foundations of Vacuum Technique,” J. Wiley, 1949.

²⁶Haas, J. M., and Gallimore, A. D., “Internal Plasma Potential Profiles in a Laboratory-Model Hall Thruster,” *Physics of Plasmas*, Vol. 8, No. 2, 2001, pp. 652–660. <https://doi.org/10.1063/1.1338535>

²⁷Peterson, P., Gallimore, A., and Haas, J., “Experimental Investigation of Hall Thruster Internal Magnetic Field Topography,” *37th Joint Propulsion Conference and Exhibit*, American Institute of Aeronautics and Astronautics. <https://doi.org/10.2514/6.2001-3890>

²⁸Frieman, J. D., Brown, N. P., Liu, C. Y., Liu, T. M., Walker, M. L. R., Khayms, V., and King, D. Q., “Electrical Facility Effects on Faraday Probe Measurements,” *Journal of Propulsion and Power*, Vol. 34, No. 1, 2018, pp. 267–269. <https://doi.org/10.2514/1.B36467>

²⁹Brown, D. L., and Gallimore, A. D., “Evaluation of Facility Effects on Ion Migration in a Hall Thruster Plume,” 2011. <https://doi.org/10.2514/1.54143>

³⁰Xu, K. G., “Ion Collimation and In-Channel Potential Shaping Using in-Channel Electrodes for Hall Effect Thrusters,” 2012. Retrieved 31 March 2024. <http://hdl.handle.net/1853/44830>